Heating of the magnetic ion system in (Zn, Mn)Se/(Zn, Be)Se semimagnetic quantum wells by means of photoexcitation

D. Keller, D. R. Yakovlev,* B. König, W. Ossau, Th. Gruber,† A. Waag,† and L. W. Molenkamp
Physikalisches Institut der Universität Würzburg, 97074 Würzburg, Germany

A. V. Scherbakov
A. F. Ioffe Physico-Technical Institute, Russian Academy of Sciences, 194021 St. Petersburg, Russia
(Received 6 July 2001; published 19 December 2001)

Heating of the spin system of magnetic Mn ions by means of photoexcited carriers has been studied in undoped (Zn, Mn)Se/(Zn, Be)Se multiple quantum well structures. Elevated spin temperature of the magnetic ions has been documented by a suppression of the giant Zeeman splitting of excitonic states measured in photoluminescence and reflectivity spectra. Low densities of photoexcitation (about 1 W/cm^2) induce strong heating of the Mn spin system. The heating shows a strong dependence on the Mn content varying from 0.004 to 0.06. It decreases with increasing Mn content due to the shortening of the spin-lattice relaxation time.

DOI: 10.1103/PhysRevB.65.035313 PACS number(s): 78.20.Ls, 75.50.Pp, 75.30.Et, 71.35.Ji

I. INTRODUCTION

Diluted magnetic (or semimagnetic) semiconductors (DMS's) provide unique opportunities for manipulation of carrier spins due to the strong *sp-d* exchange interaction between carriers (electrons or holes) and localized spins of magnetic ions. A variety of magnetic, magneto-optical, and magnetotransport phenomena makes DMS's a very reliable model system for spintronic devices. Recently the electrical injection of spin-oriented electrons from (Zn, Mn, Be)Se into GaAs has been realized.[1]

The presence of free carriers in semiconducting materials is an important issue for device application. Properties of undoped wide-gap II-VI DMS materials [e.g., (Cd, Mn)Te, (Zn, Mn)Se,...] and their heterostructures have been investigated in great detail during the last 20 years. However, experimental information about the effects induced by the presence of free carriers in these materials is very limited. In the papers addressing this issue it was shown that the system of free carriers plays an important role in the energy transfer between the phonon system (lattice) and the magnetic ion system.[2] The spin-lattice relaxation rate of the magnetic ions is accelerated by an order of magnitude in the presence of a rather diluted electron gas with a density below 10^{11} cm^{-2}.[3,4] The excess energy of free carriers gained from photoexcitation or electrical fields is transferred by means of a spin-flip exchange scattering into the magnetic ion system very efficiently.[2] This results in a heating of the localized spin system, whose temperature can exceed the lattice temperature by 200 K under high-density photoexcitation conditions.[5,6] These studies were limited to $Cd_{1-x}Mn_xTe$-based quantum wells (QW's) and to two Mn contents $x=0.01$ and 0.03 only. In the present paper we extend the investigation on $Zn_{1-x}Mn_xSe$-based heterostructures with the aim to analyze the dependence of the heating effect on the Mn concentration in detail. This is important, because it is known that the spin-lattice relaxation rate in Mn-based II-VI DMS's is a strong function of the Mn content.[7,8]

Magneto-optical properties of $Zn_{1-x}Mn_xSe$ are well known (see, e.g., Refs. 9 and 10). They are similar to the properties of the widely studied $Cd_{1-x}Mn_xTe$ system. $Zn_{1-x}Mn_xSe$/ZnSe heterostructures have been fabricated by molecular-beam epitaxy and investigated by several groups.[11–16] Due to the band-gap bowing of $Zn_{1-x}Mn_xSe$,[17] this material in combination with ZnSe serves as a quantum well for $x<0.04$ and as barriers for $x>0.04$. However for $x<0.04$ the confinement potentials for carriers are rather small. They can be overcome by the giant Zeeman splitting of band states in external magnetic fields, which leads to the formation of spin superlattices.[16,18,19] With the ternary alloy $Zn_{1-y}Be_ySe$ as a barrier material, a strong confinement of carriers in $Zn_{1-x}Mn_xSe$ can be realized for a wider range of Mn content and magnetic fields.[16]

In this paper we report on the modification of the magnetic and magneto-optical properties of $Zn_{1-x}Mn_xSe/Zn_{1-y}Be_ySe$ quantum wells under photoexcitation. Samples with different Mn content varying from 0.004 up to 0.06 have been examined by means of polarized photoluminescence and light reflectivity techniques. It was found that relatively small excitation densities cause a strong suppression of the giant Zeeman splitting of excitons. This effect evidences the heating of the Mn ion system, which is a strong function of the Mn content.

The paper is organized as follows: Sec. II describes details of the sample design and the experimental setup. In Sec. III we present experimental data and results. The discussion and summary of our findings are given in Sec. IV.

II. EXPERIMENTAL DETAILS

We have studied three $Zn_{1-x}Mn_xSe/Zn_{1-y}Be_ySe$ multiple-quantum-well structures with different Mn contents $x=0.004$, 0.012, and 0.06. All samples were fabricated by molecular-beam epitaxy on (100)-oriented GaAs substrates. Sample parameters are collected in Table I. For samples 1 ($x=0.004$) and 2 ($x=0.012$), the substrate was covered by a buffer made of 10-Å-thick BeTe, 20-Å-thick ZnSe, and a 4000-Å-thick $Zn_{0.97}Be_{0.03}Se$ layer to improve the surface

TABLE I. Parameters of $Zn_{1-x}Mn_xSe/Zn_{1-y}Be_ySe$ quantum well structures.

Sample No.	Mn content, x	Be content, y	QW width, Å	Barrier width, Å	Number of periods	X energy, eV	X FWHM, meV	S_{eff}	T_0, K
#1	0.004	0.06	100	200	5	2.8172	1.5	2.43	0.2
#2	0.012	0.06	100	200	5	2.8154	1.9	2.21	0.5
#3	0.06	0.05	100	200	10	2.8186	1.9	1.35	1.9

quality and the lattice matching with the barrier material. On this buffer layer five periods of 200-Å-thick $Zn_{0.94}Be_{0.06}Se$ barriers with an energy gap of 2.97 eV and 100-Å-thick $Zn_{1-x}Mn_xSe$ wells were grown. The structures were capped with a 300-Å-thick $Zn_{0.94}Be_{0.06}Se$ layer. Sample 3 ($x=0.06$) is similar to samples 1 and 2 but the only differences are that it consists of 10 quantum wells, and the Be concentration in barriers is 0.05 with an energy gap of 2.96 eV. All three samples reported here are nominally undoped. The band offsets caused by the difference in the band gaps of $Zn_{1-x}Mn_xSe$ and $Zn_{1-y}Be_ySe$ are distributed by the ratio 0.78/0.22 between the conduction and valence bands.[16]

Optical measurements were performed for samples immersed in pumped liquid helium at a temperature of 1.6 K. Magnetic fields up to 7 T were generated by a superconducting split-coil solenoid and were applied parallel to the structure growth axis and to the direction of the collected light (Faraday geometry). An Ar-ion laser operating at the wavelength of 363.8 nm served as an excitation source for the photoluminescence (PL) or as a pump source for a tunable dye laser (Stilben 3), which was used for PL excitation (PLE) and for reflectivity measurements under additional laser illumination. For reflectivity experiments, a halogen lamp was used, whose high-energy spectral range, which exceeds the band gap of $Zn_{1-y}Be_ySe$ barriers, was blocked by a selective filter to minimize possible heating of the sample and to avoid photoinduced changes of electron density in QW's. A mask with a pinhole with a diameter of 1 mm covered the samples. The sizes of the exciting laser spot and illumination lamp spot were chosen larger than the pinhole size to avoid spatially inhomogeneous excitation. Due to the optical selection rules for excitonic luminescence and absorption in the chosen Faraday geometry the detected light was either right-hand σ^+ or left-hand σ^- circularly polarized. The luminescence signal or the reflected light was dispersed by a 1-m monochromator and detected either with a charged-coupled device or a cooled photomultiplier followed by a photon counting system. The spin-lattice relaxation dynamics of magnetic ions have been measured by means of a method based on optical detection of injected nonequilibrium phonons. Details of the method are presented in Ref. 8.

III. EXPERIMENTAL RESULTS

Let us start with the description of systems of a DMS heterostructure, whose interaction determines the studied phenomena. Schematically these interacting systems, which are convenient to consider as energy reservoirs characterized by heat capacity and temperature, are shown in Fig. 1. They are (i) the phonon system (i.e., the lattice), (ii) the magnetic ion system [the Mn ion system in the case of (Zn, Mn)Se-based heterostructures], and (iii) the carriers, which are photoexcited in the studied case of undoped structures. The photocarriers generated by light absorption have an excess energy and a finite lifetime limited by various recombination processes. Via spin-flip exchange scattering the photocarriers pass their excess energy into the Mn system and elevate its spin temperature.[2] The energy flux from the Mn system to the lattice is determined by the spin-lattice relaxation (SLR). In very diluted systems with $x<0.01$, where Mn ions are isolated entities, the spin-lattice relaxation rate is extremely low. However, it increases by several orders of magnitude with a growing concentration of Mn ions, when clusters of magnetic ions are formed.[7] Under the influence of steady-state photoexcitation, the resulting temperature of the magnetic ion system T_{Mn} will exceed the lattice temperature (i.e., the bath temperature) T_L. The temperature difference is determined by the energy flux supplied by photocarriers and the SLR rate.

Figure 2 shows a survey of photoluminescence, PL excitation, and reflectivity spectra for the three samples studied. The structures differ in Mn content of the QW layers, but the range of x variations is relatively small and does not exceed 0.06. As a result the optical spectra of all three samples are very similar. We will describe them with the example of sample 2 with $x=0.012$ shown in Fig. 2(b). Two strong resonances corresponding to the exciton (X) ground states involving heavy holes ($1s$-hh) and light holes ($1s$-lh) are clearly seen in the reflectivity spectrum. They are split by 14 meV due to the strain and quantum confinement effects. Both excitonic resonances are observable as strong lines in the PL

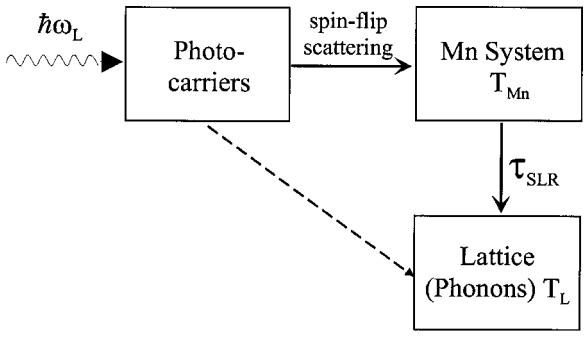

FIG. 1. Scheme of the energy reservoirs of DMS heterostructures, which participate in the Mn heating process. Photocarriers created by light of energy $\hbar\omega_L$ transfer their energy to the Mn system and to the lattice. Solid arrows denote relaxation channels responsible for the energy exchange with the magnetic ion system. τ_{SLR} denotes the spin-lattice relaxation time.

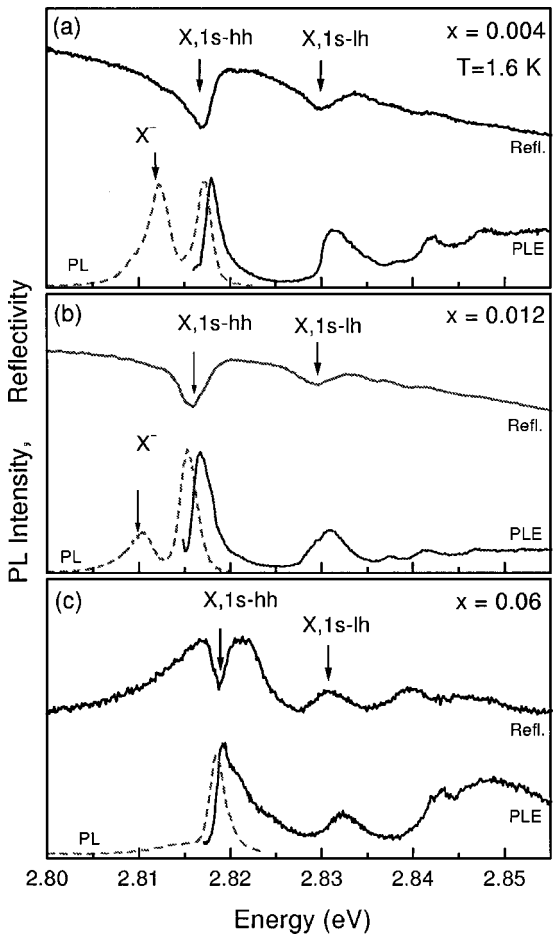

FIG. 2. Photoluminescence, PL excitation, and reflectivity spectra of $Zn_{1-x}Mn_xSe/Zn_{1-y}Be_ySe$ QW's at $T=1.6$ K and in the absence of magnetic field. Resonances of heavy-hole ($1s$-hh) and light-hole ($1s$-lh) excitons are marked by arrows. (a) Sample 1 with $Zn_{0.996}Mn_{0.004}Se$ QW's (b) sample 2 with $Zn_{0.988}Mn_{0.012}Se$ QW's, and (c) sample 3 with $Zn_{0.94}Mn_{0.06}Se$ QW's.

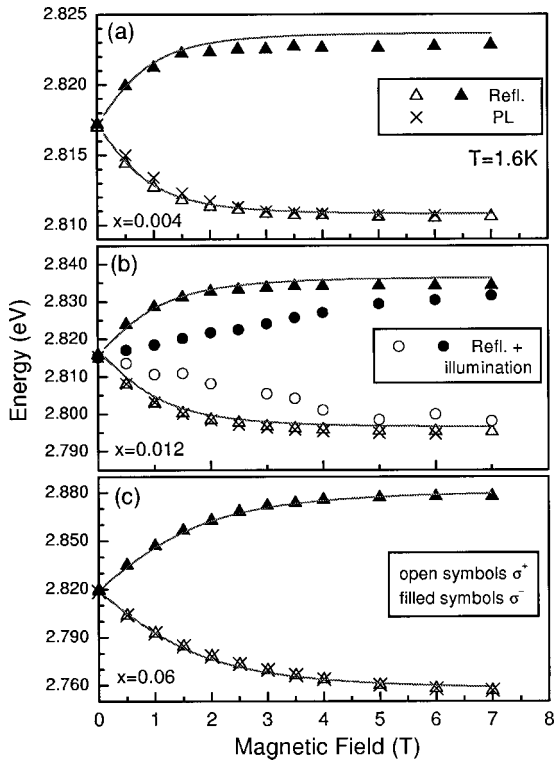

FIG. 3. Giant Zeeman splitting of the heavy-hole excitons in $Zn_{1-x}Mn_xSe/Zn_{1-y}Be_ySe$ QW's. Experimental data are shown by symbols (open for σ^+ polarization and closed for σ^- polarization). Triangles are for reflectivity and crosses for photoluminescence data taken under a very low photoexcitation density of 0.016 W/cm^2. Circles represent exciton energies in reflectivity measurements with additional creation of carriers by laser illumination ($\hbar\omega_L=3.4$ eV, $P=0.7$ W/cm^2). Reduction of the Zeeman splitting caused by the heating of the Mn system is clearly seen. Solid lines represent the best fit for the reflectivity data points measured without additional illumination (i.e., for the cold Mn system) along the procedure described in the text. Mn concentration values have been determined from this fit.

excitation spectrum. The photoluminescence spectrum consists of two lines. The line at 2.8154 eV is due to the recombination of heavy-hole excitons. The small full width at half maximum of this line of 1.9 meV indicates a high structural quality of the sample. Its Stokes shift from the PLE maximum does not exceed 1.4 meV, which allows us to conclude that the nonmagnetic localization of excitons on alloy and QW width fluctuations, and their magnetic localization, caused by the magnetic polaron formation,[20,21] do not play a significant role in this structure. Another emission line shifted by 4.9 meV to lower energy from the exciton line corresponds to the negatively charged exciton (trion) X^-, which is a complex of two electrons bound to one hole. The binding energy of the trion of 4.9 meV is in good agreement with literature data for ZnSe-based QW's.[22,23] Due to the band-gap bowing in $Zn_{1-x}Mn_xSe$,[17] excitonic resonances in samples 1 and 3 have slightly higher energies compared to sample 2 (see Table I).

In external magnetic fields, excitonic transitions experience a giant Zeeman splitting caused by the strong exchange interaction of carriers with the localized magnetic moments of the Mn ions. A survey of the exciton Zeeman splitting determined from reflectivity and PL spectra for the three samples is presented in Fig. 3. In order to avoid heating of the Mn system, PL spectra were measured under very low photoexcitation density $P=0.016$ W/cm^2 (shown by crosses). These data points coincide very well with the reflectivity data detected without additional illumination (triangles). In order to determine the Mn concentration in the studied samples we apply a commonly used approach for the description of the giant Zeeman splitting effect, in which the value of x is used as a fitting parameter.

In the mean-field approximation the energy of QW excitons with the total spin ±1 is described by (after Refs. 24 and 2)

$$E_X^{\pm1}(B)=E_X(B=0)\pm\tfrac{1}{2}(\delta_e\alpha-\delta_h\beta)N_0x\langle S_z\rangle, \qquad (1)$$

where $E_X(B=0)$ is the exciton energy in the absence of external magnetic field B, and $N_0\alpha=0.26$ and $N_0\beta=-1.31$ eV are the exchange constants for the conduction

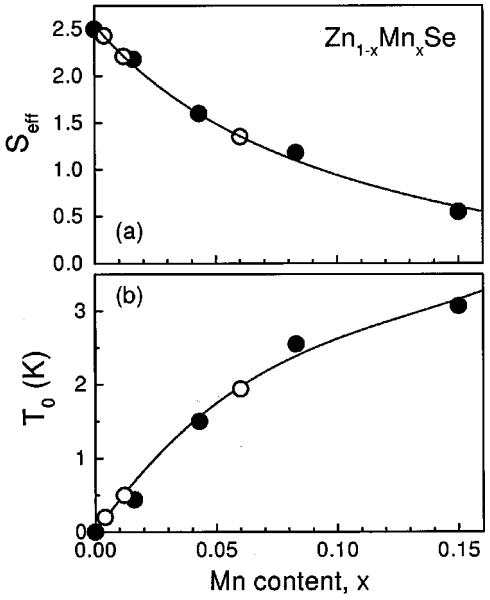

FIG. 4. Phenomenological parameters S_{eff} and T_0 for $Zn_{1-x}Mn_xSe$ determined experimentally in Ref. 10 (closed symbols). Interpolation of these data points is shown by solid lines. Parameters corresponding to the best fit of the giant Zeeman splitting of exciton states in $Zn_{1-x}Mn_xSe/Zn_{1-y}Be_ySe$ QW's are shown by open symbols.

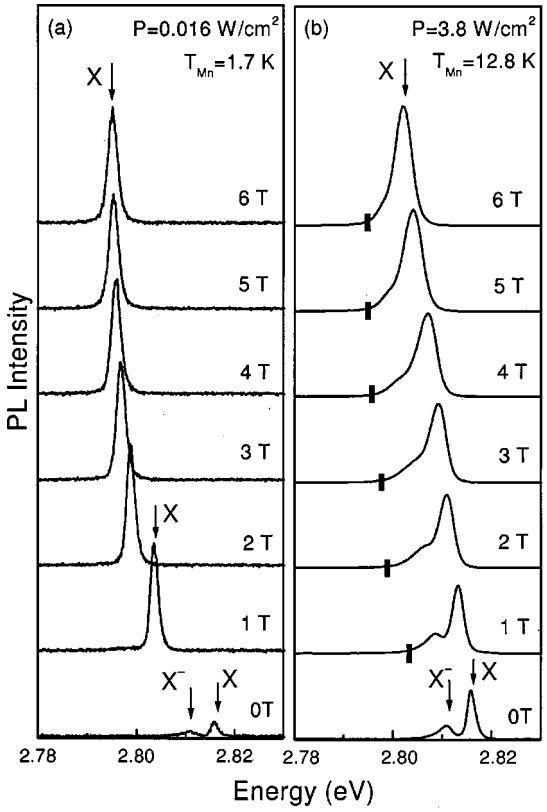

FIG. 5. Comparison of photoluminescence spectra of the sample 2 ($x=0.012$) detected in different magnetic fields for two excitation densities: (a) $P=0.016\ \text{W/cm}^2$, and (b) $P=3.8\ \text{W/cm}^2$, $T=1.6$ K. Exciton (X) and negatively charged exciton (X^-) lines are marked by arrows. Bold bars in (b) trace the excitonic energies detected in (a) i.e., they correspond to the exciton energy in the case of the cold Mn system with $T_{\text{Mn}}=1.7$ K. T_{Mn} was derived from a fitting of the Zeeman splitting, treating T_{Mn} as a fitting parameter (see Fig. 6).

and valence band, respectively, in $Zn_{1-x}Mn_xSe$.[25] N_0 is the inverse unit-cell volume and x is the Mn mole fraction. δ_e and δ_h are parameters that account for the leakage of the electron and hole wave functions into the nonmagnetic barriers. In the studied samples $\delta_e=\delta_h=0.96$, i.e., 96% of carrier wave functions are localized in the DMS layers of QW's. These parameters have been calculated from the hole and electron envelope wave function, with a valence-band offset of 0.22.[16] $\langle S_z\rangle$ represents the thermal average value of the Mn spin along the direction of magnetic field $B=B_z$ at a Mn spin temperature T_{Mn}. It can be expressed by the modified Brillouin function $B_{5/2}$,

$$\langle S_z\rangle = -S_{\text{eff}}(x)B_{5/2}\left[\frac{5g_{\text{Mn}}\mu_B B}{2k_B(T_{\text{Mn}}+T_0(x))}\right]. \qquad (2)$$

Here $g_{\text{Mn}}=2$ is the g factor of the Mn d state. S_{eff} and T_0 are parameters for the effective spin and effective temperature of the Mn ions that phenomenologically describe the effect of the antiferromagnetic Mn-Mn exchange interaction. Functional dependencies of these parameters on x value based on the data for $Zn_{1-x}Mn_xSe$ epilayers after Ref. 10 are plotted in Fig. 4 by closed circles. Continuous interpolations of these data given by $S_{\text{eff}}=-0.804+0.364/(x-0.109)$ and $T_0=47.2x-281x^2+714x^3$ are shown by lines. These functions were used in the fitting of the Zeeman splitting to derive the Mn content x for the studied structures. The results of the best fit, where x was the only fitting parameter and T_{Mn} was taken to be equal to the lattice temperature of 1.6 K, are represented by solid lines in Fig. 3. The values of x, S_{eff}, and T_0 determined for the studied samples are collected in Table I and shown in Fig. 4 by open symbols.

We turn now to experiments in which a heating of the Mn system by means of photoexcitation was found. Figure 5 compares PL spectra of sample 2 measured in magnetic fields for two densities of photoexcitation, which differ by about two orders of magnitude. For very low excitation density of 0.016 W/cm^2 [Fig. 5(a)] both X and X^- lines are present in the PL spectrum at zero magnetic field. At a magnetic field of 1 T the trion luminescence is totally suppressed and only the exciton line is visible. The mechanism of suppression has been discussed in Refs. 26 and 16. In short, when the giant Zeeman splitting of the electron state in the conduction band exceeds the binding energy of the trion, the trion state becomes unstable. Under these conditions the exciton becomes the bound state of the system with the lowest energy. The same mechanism is responsible for the suppression of the donor-bound exciton lines with increasing magnetic fields reported for bulk DMS's.[27] The field-induced low-energy shift of the exciton line coincides very well with the shift of the exciton resonance in reflectivity spectra [see also Fig. 3(b)]. From that fact we conclude that under such low photoexcitation density the Mn system stays cold. Indeed the temperature of the Mn system determined under these conditions from the fit of the Zeeman shift T_{Mn}

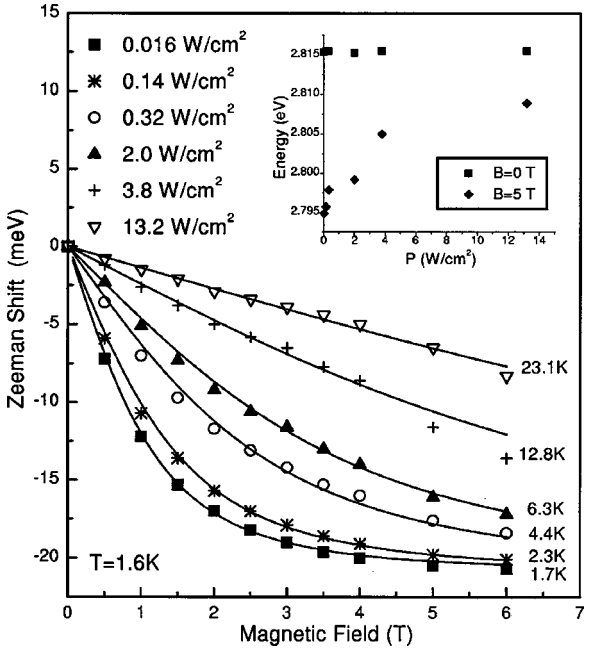

FIG. 6. The giant Zeeman shift of excitons in sample 2 ($x=0.012$) evaluated from PL spectra measured under different excitation densities. Lines represent the fit of the experimental data. Determined T_{Mn} values are given in the figure. In the inset, the dependence of the exciton energy on excitation density is shown for two magnetic fields.

$=1.7\,\mathrm{K}$ differs negligibly from the bath temperature $T=1.6\,\mathrm{K}$.

Figure 5(b) presents PL spectra, recorded with a laser power density of 3.8 W/cm^2. The vertical bars mark the position of the exciton line for the low excitation density taken from Fig. 5(a). It is clearly seen that the giant Zeeman shift of the exciton line is strongly reduced by increasing the power density. For example, at $B=2\,\mathrm{T}$ it is 5.1 meV, which is only 30% of the energy shift at the lower power density of 17.1 meV. T_{Mn} is the only parameter in Eqs. (1) and (2) that can be affected by photoexcitation. Obviously, the observed changes can be explained by a heating of the Mn system, i.e., an increase of T_{Mn}. Indeed the shift of the exciton energy is well described by Eqs. (1) and (2) using $T_{\mathrm{Mn}}=12.8\,\mathrm{K}$ (see Fig. 6 with the crosses and corresponding fit shown by line).

We would like to stress here that the observed suppression of the giant Zeeman splitting by photoexcitation is a general phenomenon that is not related to the specifics of photoluminescence detection (i.e., localization mechanisms, spectral diffusion in the tail of localized states, dynamics of recombination, energy relaxation, etc.). We detected this effect in PL excitation spectra and in reflectivity spectra with additional creation of photoexcited carriers by laser illumination ($\hbar\omega_L=3.4\,\mathrm{eV}$), as well. Circles in Fig. 3(b) represent results for the latter case with illumination density of 0.7 W/cm^2. The symmetric suppression of the giant Zeeman splitting for both spin components of the exciton state can be seen clearly. We have checked also that the laser illumination has no effect on the giant Zeeman splitting, when the photon energy is smaller than the exciton energy ($\hbar\omega_L=2.72\,\mathrm{eV}$). Excitation densities up to 10 W/cm^2 have been applied without any observable changes in the Zeeman splitting. This confirms that the creation of photocarriers in $Zn_{1-x}Mn_xSe/Zn_{1-y}Be_ySe$ heterostructures is essential for the heating of the Mn system. Other mechanisms of heating caused by laser light absorption in the $Zn_{1-x}Mn_xSe/Zn_{1-y}Be_ySe$ heterostructures and/or in the GaAs substrate give no significant contribution in the used experimental conditions. It is worthwhile to note that for $P=3.8\,\mathrm{W/cm^2}$, the trion line in PL spectra disappears at higher magnetic fields compared with the case of $P=0.016\,\mathrm{W/cm^2}$ [see Fig. 5(b)], which can be explained by a decrease of the electron Zeeman splitting.

In more detail the effect of the photoexcitation density on the giant Zeeman shift of the exciton line in sample 2 is displayed in Fig. 6. Experimental data detected for different excitation densities were fitted along the procedure described above in order to evaluate the temperature of the Mn system. Obviously the Mn system can be heated to high temperatures of 23 K by means of relatively low excitation densities of 13 W/cm^2. We note here that in the whole range of magnetic fields up to 6 T very reliable fits can be achieved with a Mn temperature, which is independent of the magnetic field. This differs from the experimental appearances in (Cd, Mn)Te-based QW's with a two-dimensional electron gas, where the heating of the Mn system varies with the magnetic-field values.[16] In this case T_{Mn} shows a strong dependence on the magnetic field, caused by the presence of the degenerated two-dimensional electron gas. The dependence of the exciton energy on excitation density in the case of zero magnetic field is compared to the case of an applied magnetic field in the inset of Fig. 6. At $B=5\,\mathrm{T}$ the exciton energy shows a strong increase with an increase of the laser power, whereas at $B=0\,\mathrm{T}$ the energy is independent of the photoexcitation density. From this fact we conclude that the variation of the exciton energy under increasing photoexcitation density is dominated by the suppression of the giant Zeeman splitting. Other possible mechanisms caused by, e.g., magnetic polaron suppression or narrowing of the band gap for evaluated lattice temperatures are not detectable in the studied structures.

We have found that the heating efficiency strongly depends on the Mn concentration. Figure 7 compares $T_{\mathrm{Mn}}(P)$ dependencies ($\hbar\omega_L=3.4\,\mathrm{eV}$) measured at $B=1.5\,\mathrm{T}$ for the three samples studied. For sample 1 with $x=0.004$, T_{Mn} reaches 42 K at $P=4.5\,\mathrm{W/cm^2}$, which corresponds to a suppression of the giant Zeeman shift down to 10% of its value at $T_{\mathrm{Mn}}=1.6\,\mathrm{K}$. However, an increase of the Mn content leads to a strong suppression of the heating efficiency. At $P\approx4.5\,\mathrm{W/cm^2}$ the Mn temperature decreases from 42 to 3.2 K when x increases from 0.004 to 0.06.

We have also checked that for the studied structures and for the used experimental conditions the heating efficiency of the Mn system is rather independent of the energy of photoexcitation and is insensitive to changes from above-barrier to below-barrier excitation energies. In the inset of Fig. 7 the Mn heating for above-barrier ($\hbar\omega_L=3.4\,\mathrm{eV}$) and below-barrier ($\hbar\omega_L=2.85\,\mathrm{eV}$) excitations are compared at $B=1.5\,\mathrm{T}$. The same focusing conditions have been chosen for above-barrier and below-barrier excitations. To avoid the dif-

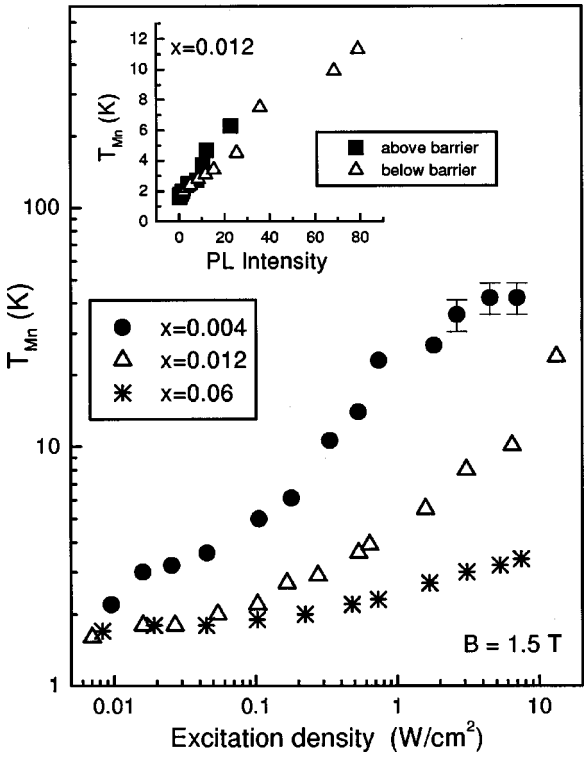

FIG. 7. Mn temperature plotted against excitation density for $Zn_{1-x}Mn_xSe/Zn_{1-y}Be_ySe$ structures with different Mn content x at a magnetic field of $B=1.5$ T. Excitation energy with $\hbar\omega_L=3.4$ eV exceeds the energy gap of barriers. $T=1.6$ K. Inset compares Mn heating for sample 2 for above-barrier ($\hbar\omega_L=3.4$ eV) and below-barrier photoexcitations ($\hbar\omega_L=2.837$ eV) at $B=1.5$ T.

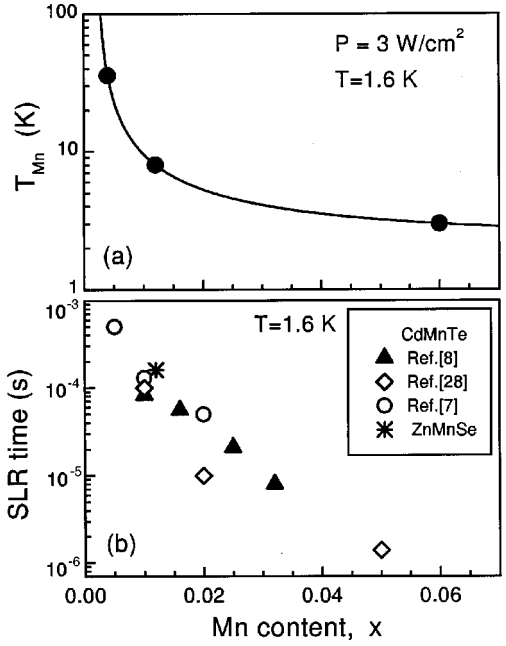

FIG. 8. (a) Temperature of the Mn system vs Mn content determined for $Zn_{1-x}Mn_xSe/Zn_{1-y}Be_ySe$ structures under constant photoexcitation density $P=3.0$ W/cm^2. $T=1.6$ K. Line is given as a guide for the eye. (b) Spin-lattice relaxation time vs Mn content for undoped $Cd_{1-x}Mn_xTe$ bulk samples (Refs. 7 and 28) and $Cd_{1-x}Mn_xTe$-based heterostructures (Ref. 8). Star shows a data point for sample 2 ($x=0.012$) measured by means of the injection of nonequilibrium phonons.

ficulties caused by the differences in light absorption and to properly account for carrier collection from the barriers into the QW, the Mn temperature is plotted as a function of integral PL intensity from the QW, which in turn is proportional to the number of electron-hole pairs in the QW. One can see that dependencies measured under various excitation conditions coincide reasonably well with each other.

To illustrate the decrease of the heating efficiency with the growing Mn content we have plotted a dependence $T_{\mathrm{Mn}}(x)$ in Fig. 8(a). This dependence has been detected at a constant photoexcitation density $P=3.0$ W/cm^2. At higher Mn contents the magnetic ion system becomes much stronger coupled to the lattice, which is documented by the strong decrease of the SLR time shown in Fig. 8(b). We present here literature data for $Cd_{1-x}Mn_xTe$ bulk materials and $Cd_{1-x}Mn_xTe/Cd_{1-y}Mg_yTe$ heterostructures,[7,8,28] where the properties of the Mn ion system are very similar to those in $Zn_{1-x}Mn_xSe$. We have measured SLR time (τ_{SLR}) in sample 2 [shown by a star in Fig. 8(b)] using a technique based on the injection of nonequilibrium phonons (for details see Ref. 8). In an undoped $Zn_{0.988}Mn_{0.012}Se/Zn_{0.94}Be_{0.06}Se$ QW structure the SLR time is about 160 μs at $B=2$ T and $T=1.6$ K. This value is very close to $\tau_{\mathrm{SLR}}=70\,\mu$s measured for undoped $Cd_{0.988}Mn_{0.012}Te$ at the same conditions. We suppose that the strong dependence $\tau_{\mathrm{SLR}}(x)$ established for $Cd_{1-x}Mn_xTe$ is also valid for $Zn_{1-x}Mn_xSe$. We believe that this is the dominating factor, which controls the heating efficiency in DMS heterostructures. We will discuss this in more detail in the next section.

We have also used an alternative optical technique to detect variations of T_{Mn} and to register the heating of the Mn system. This technique is based on the analysis of the circular polarization degree of photoluminescence, which is induced by external magnetic fields. It allows tracing small variations of magnetization in DMS heterostructures with high accuracy.[29,30] The circular polarization degree P_c of the luminescence is

$$P_c=\frac{I_+-I_-}{I_++I_-}, \tag{3}$$

where I_+ and I_- correspond to the intensity of luminescence with σ^+ and σ^- polarization, respectively. In external magnetic fields, $P_c(B)$ dependence is caused by the thermal population of the exciton spin sublevels split due to the giant Zeeman effect by the value $\Delta E_Z(B,T_{\mathrm{Mn}})$.

$$P_c(B)=\frac{\tau}{\tau+\tau_S}\tanh\left(\frac{\Delta E_Z(B,T_{\mathrm{Mn}})}{2k_BT_X}\right), \tag{4}$$

where τ and τ_S is the exciton lifetime and spin-relaxation time, respectively. T_X is the temperature of thermalized excitons contributing to radiative recombination. Under low and moderate excitation densities used in our experiments, T_X does not differ significantly from the bath temperature. In

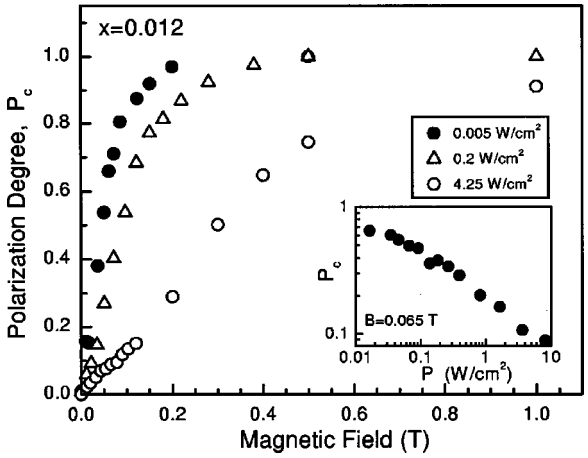

FIG. 9. Magnetic-field-induced circular polarization of PL in sample 2 ($x=0.012$) detected for different densities of photoexcitation: 0.005, 0.2, and 4.25 W/cm^2. $T=1.6$ K. In the inset, the dependence of polarization degree on the excitation density is plotted.

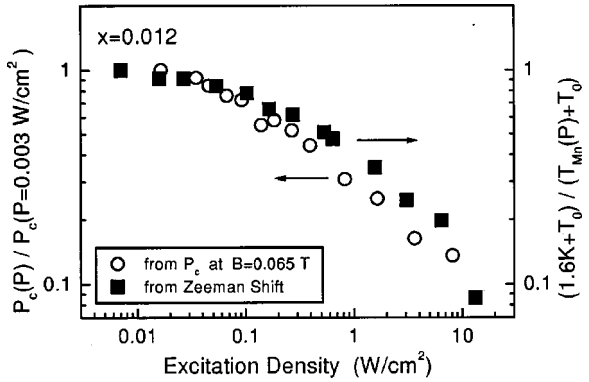

FIG. 10. Comparison of two parameters that characterize the heating of the Mn system with increasing density of photoexcitation for sample 2 ($x=0.012$): (i) The degree of magnetic-field-induced circular polarization of PL P_c, measured at $B=0.065$ T (circles) and (ii) $(T_{\mathrm{Mn}}+T_0)^{-1}$ derived directly by fitting of the giant Zeeman shift of exciton PL lines (squares). The parameters are normalized to their (maximal) values at the lowest excitation density.

DMS's $\tau_S \ll \tau$ due to the strong exchange interaction of excitons with the localized spins of magnetic ions. As a result $\tau/(\tau+\tau_S)\approx 1$.

There are several advantages of the polarization technique, compared to deriving T_{Mn} from the Zeeman shift of excitons. First, it is very sensitive at very low magnetic fields down to 0.01 T, where the Zeeman splitting is not resolvable, especially in structures with a large inhomogeneous broadening of the exciton lines. Second, the technique can be applied to structures with very large inhomogeneous broadening, because it is dealing with the PL intensities rather than with the spectral splitting of PL lines. According to Eq. (4) the sensitivity in determination of changes in ΔE_Z is limited by the $k_B T_X$ value, which for $T_X=1.6$ K is better than 0.2 meV. However, the polarization technique is not universal. It cannot be used in high magnetic fields, where P_c saturates at its maximum value. Also the extraction of absolute values of ΔE_Z and T_{Mn} is often complicated due to the possible contribution of magnetic fluctuations and magnetic polaron formation.[30,31] In this paper the polarization technique was used to investigate the heating of the Mn system at weak magnetic fields.

Figure 9 shows the polarization degree $P_c(B)$ for sample 2 for different excitation densities. The polarization degree increases linearly with growing magnetic fields with saturation at a level of 1.0, which corresponds to the full polarization of excitons. For the lowest excitation density $P=0.005$ W/cm^2, the full polarization is achieved at a magnetic field of 0.2 T. The initial slope of $P_c(B)$ dependencies decreases for higher excitation densities, which evidences the decreasing of $\Delta E_Z(B,T_{\mathrm{Mn}})$ under elevated temperatures of the Mn system. The dependence of P_c on the density of photoexcitation measured at a magnetic field of 0.065 T is displayed in the inset of Fig. 9. The monotonic decrease of the polarization degree was detected in the whole range of applied excitation densities.

Results of the two optical techniques are compared in Fig. 10. The P_c data from the inset of Fig. 9 were normalized on the polarization degree value at the lowest excitation density and plotted in Fig. 10 by open circles. This dependence is compared with the $T_{\mathrm{Mn}}(P)$ results taken from Fig. 7, which have been converted to the form of $[T_{\mathrm{Mn}}(P)+T_0]^{-1}$. The reason for that is that at a low magnetic field of 0.065 T, $\Delta E_Z/2k_BT_X \ll 1$ is valid and Eq. (4) can be approximated to $P_c \approx \Delta E_Z/2k_BT_X$. In turn it follows from Eqs. (1) and (2) that $\Delta E_Z \propto (T_{\mathrm{Mn}}+T_0)^{-1}$. As a result we get $P_c \propto [T_X(T_{\mathrm{Mn}}+T_0)]^{-1}$. Assuming that exciton temperature T_X does not vary significantly for low and moderate excitation densities used in our experiments, one can expect $P_c(P) \propto [T_{\mathrm{Mn}}(P)+T_0]^{-1}$. Experimental results from Fig. 10 confirm that indeed the polarization technique and Zeeman shift analysis give very similar information on the temperature of the Mn system. We also conclude that the heating of the Mn system by means of photoexcitation in undoped QW's studied here is independent of the magnetic-field values.

IV. DISCUSSION

Let us discuss the experimental findings on the basis of the scheme presented in Fig. 1. We have established that the energy of laser radiation being absorbed by the system of photocarriers is efficiently transferred into the system of magnetic ions and induces its heating. There are two possible channels for this energy transfer. One is the direct energy exchange between carriers and Mn ions mediated by the strong exchange interaction. The other one is the channel bypassed by the phonon system, when the acoustical phonons generated in the process of energy relaxation of photocarriers are absorbed by the Mn ions. The latter possibility can be excluded on the basis of the following arguments. (i) The heat capacity of the phonon system is too large to achieve the phonon temperature of 40 K (which is the T_{Mn} measured for sample 1) by means of moderate excitation densities used in our experiments. (ii) If we exclude the direct heating process from consideration, the temperature of the Mn system should approach the temperature of the phonon system under the steady-state excitation condi-

tions. Also in this case we should not expect strong dependence of the heating efficiency on the Mn content, which is in conflict with the experimental data presented in Fig. 8.

Therefore, we conclude that two energy fluxes (shown by solid arrows in Fig. 1) control the temperature of the magnetic ion system under photoexcitation. The Mn system receives energy from the photocarriers via spin-flip exchange scattering[2] and looses energy via spin-lattice relaxation to the phonon system.

It was found experimentally that the heating of the Mn system is suppressed by increasing Mn content. Two reasons may explain that. With increasing Mn content, the heat capacity of the Mn system increases, too. However, we believe that a strong increase in the spin-lattice relaxation rate for higher x values gives the main contribution to the effect. The Mn system of high x interacts considerably better with the phonons and, therefore, its cooling is much more effective.

In conclusion, we have found an efficient energy transfer from photocarriers to the Mn system, which causes a heating of the magnetic ion system of the studied $Zn_{1-x}Mn_xSe/Zn_{1-y}Be_ySe$ DMS quantum wells. The heating manifests itself in a strong reduction of the Zeeman splitting of excitons. Experimentally it was detected in photoluminescence, PL excitation, and reflectivity measurements as a spectral shift of the excitonic transition, as well as a suppression of the polarization degree of excitonic emission. For samples with low Mn content ($x=0.004$) the temperature of the Mn system can reach values of 42 K at excitation densities of about 4.5 W/cm^2 (at a bath temperature of 1.6 K). An increase of the Mn content up to 0.06, however, results in a suppression of the heating. We believe that this information on the modification of magnetic properties of DMS materials in the presence of free carriers with excess kinetic energy is important for the engineering of spintronic devices based on DMS's.

ACKNOWLEDGMENTS

This work is supported by the Deutsche Forschungsgemeinschaft through Sonderforschungsbereich 410 and the NATO Grant No. PST.CLG.976858.

*Also at A. F. Ioffe Physico-Technical Institute, Russian Academy of Sciences, 194021 St. Petersburg, Russia.

†Present address: Abteilung Halbleiterphysik, Universität Ulm, 89081 Ulm, Germany.

[1] R. Fiederling, M. Keim, G. Reuscher, W. Ossau, G. Schmidt, A. Waag, and L. W. Molenkamp, Nature (London) **402**, 787 (1999).

[2] B. König, I. A. Merkulov, D. R. Yakovlev, W. Ossau, S. M. Ryabchenko, M. Kutrowski, T. Wojtowicz, G. Karczewski, and J. Kossut, Phys. Rev. B **61**, 16 870 (2000).

[3] D. R. Yakovlev, A. V. Scherbakov, B. König, W. Ossau, A. Akimov, T. Wojtowicz, G. Karczewski, and J. Kossut, *Proceedings of the 25th International Conference on the Physics of Semiconductors, Osaka, Japan 2000*, edited by N. Miura and T. Ando (Springer, Berlin, 2001), p. 252.

[4] A. V. Scherbakov, D. R. Yakovlev, A. V. Akimov, I. A. Merkulov, B. König, W. Ossau, L. W. Molenkamp, T. Wojtowicz, G. Karczewski, G. Cywinski, and J. Kossut, Phys. Rev. B **64**, 155205 (2001).

[5] M. G. Tyazhlov, A. I. Filin, A. V. Larionov, V. D. Kulakovskii, D. R. Yakovlev, A. Waag, and G. Landwehr, Zh. Eksp. Teor. Fiz. **112**, 1440 (1997) [Sov. Phys. JETP **85**, 784 (1997)].

[6] M. G. Tyazhlov, V. D. Kulakovskii, A. I. Filin, D. R. Yakovlev, A. Waag, and G. Landwehr, Phys. Rev. B **59**, 2050 (1999).

[7] D. Scalbert, Phys. Status Solidi B **193**, 189 (1996).

[8] A. V. Scherbakov, A. V. Akimov, D. R. Yakovlev, W. Ossau, G. Landwehr, T. Wojtowicz, G. Karczewski, and J. Kossut, Phys. Rev. B **62**, R10 641 (2000).

[9] O. Goede and W. Heimbrodt, Phys. Status Solidi B **146**, 11 (1988).

[10] W. Y. Yu, A. Twardowski, L. P. Fu, A. Petrou, and B. T. Jonker, Phys. Rev. B **51**, 9722 (1995).

[11] J. Warnock, B. T. Jonker, A. Petrou, W. C. Chou, and X. Lui, Phys. Rev. B **48**, 17 321 (1993).

[12] N. Dai, L. R. Ram-Mohan, H. Luo, G. L. Yang, F. C. Zhang, M. Dobrowolska, and J. K. Furdyna, Phys. Rev. B **50**, 18 153 (1994).

[13] E. Deleporte, T. Lebihen, B. Ohnesorge, Ph. Roussignol, C. Delalande, S. Guha, and H. Munekata, Phys. Rev. B **50**, 4514 (1994).

[14] P. J. Klar, D. Wolverson, J. J. Davies, W. Heimbrodt, and M. Happ, Phys. Rev. B **57**, 7103 (1998).

[15] V. V. Rossin, F. Heneberger, and J. Puls, Phys. Rev. B **53**, 16 444 (1996).

[16] B. König, U. Zehnder, D. R. Yakovlev, W. Ossau, T. Gerhard, M. Keim, A. Waag, and G. Landwehr, Phys. Rev. B **60**, 2653 (1999).

[17] A. Twardowski, T. Dietl, and M. Demianiuk, Solid State Commun. **48**, 845 (1983).

[18] N. Dai, H. Luo, F. C. Zhang, N. Samarth, M. Dobrowolska, and J. K. Furdyna, Phys. Rev. Lett. **67**, 3824 (1991).

[19] B. T. Jonker, H. Abad, L. P. Fu, W. Y. Yu, A. Petrou, and J. Warnock, J. Appl. Phys. **75**, 5725 (1994).

[20] G. Mackh, M. Hilpert, D. R. Yakovlev, W. Ossau, H. Heinke, T. Litz, F. Fischer, A. Waag, G. Landwehr, R. Hellmann, and E. O. Göbel, Phys. Rev. B **50**, 14 069 (1994).

[21] D. R. Yakovlev and K. V. Kavokin, Comments Condens. Matter Phys. **18**, 51 (1996).

[22] G. V. Astakhov, D. R. Yakovlev, V. P. Kochereshko, W. Ossau, J. Nürnberger, W. Faschinger, and G. Landwehr, Phys. Rev. B **60**, R8485 (1999).

[23] G. V. Astakhov, V. P. Kochereshko, D. R. Yakovlev, W. Ossau, J. Nürnberger, W. Faschinger, and G. Landwehr, Phys. Rev. B **62**, 10 345 (2000).

[24] J. A. Gaj, R. Planel, and G. Fishman, Solid State Commun. **29**, 435 (1979).

[25] A. Twardowski, M. von Ortenberg, M. Demianiuk, and R. Pauthenet, Solid State Commun. **51**, 849 (1984).

[26] S. I. Gubarev, V. D. Kulakovskii, M. G. Tyazhlov, D. R. Yakovlev, A. Waag, and G. Landwehr, Ann. Phys. (Paris) **20**, C2-137 (1995).

[27] D. Heiman, P. Becla, R. Kershaw, D. Ridgley, K. Dwight, A. Wold, and R. R. Galazka, Phys. Rev. B **34**, 3961 (1986).

[28] W. Farah, D. Scalbert, and M. Nawrocki, Phys. Rev. B **53**, R10 461 (1996).

[29] V. P. Kochereshko, G. R. Pozina, I. A. Merkulov, D. R. Yakovlev, G. Landwehr, W. Ossau, and A. Waag, Pis'ma Zh. Eksp. Teor. Fiz. **61**, 390 (1995) [JETP Lett. **61**, 396 (1995)].

[30] D. R. Yakovlev, U. Zehnder, W. Ossau, A. Waag, G. Landwehr, T. Wojtowicz, G. Karczewski, and J. Kossut, J. Magn. Magn. Mater. **191**, 25 (1999).

[31] I. A. Merkulov, D. R. Yakovlev, K. V. Kavokin, G. Mackh, W. Ossau, A. Waag, and G. Landwehr, Pis'ma Zh. Eksp. Teor. Fiz. **62**, 313 (1995) [JETP Lett. **62**, 335 (1995)].